Analysis of Electron Donor-Acceptor Complexes: $H_3N{\cdot}F_2$, $H_3N{\cdot}Cl_2$, and $H_3N{\cdot}ClF$

I. Røeggen* and T. Dahl

Contribution from the Institute of Mathematical and Physical Sciences, University of Tromsø, 9000 Tromsø, Norway. *Received March 5, 1991*

Abstract: An extended geminal model has been applied to study the electron donor-acceptor complexes $H_3N{\cdot}F_2$, $H_3N{\cdot}Cl_2$, and $H_3N{\cdot}ClF$. By adopting a [9s, 6p, 2d/7s, 4p, 2d/4s, 2p] contracted Gaussian-type basis set, the equilibrium N-X (X = nearest halogen atom) distances are predicted to be 2.76 Å ($H_3N{\cdot}F_2$), 2.57 Å ($H_3N{\cdot}Cl_2$), and 2.30 Å ($H_3N{\cdot}ClF$). The predicted binding energies are 6.8 kJ/mol ($H_3N{\cdot}F_2$), 24.6 kJ/mol ($H_3N{\cdot}Cl_2$), and 45.1 kJ/mol ($H_3N{\cdot}ClF$). An energy decomposition analysis demonstrates the similarity between these three complexes. The Coulombic interaction between the distorted monomers is found to be the main origin of the intermolecular interaction. A decomposition of the Coulombic term into electrostatic and inductive terms shows that the latter is approximately 4 times larger than the former for all the three complexes.

I. Introduction

Molecular complexes between amines and halogens belong to the class of complexes called charge-transfer complexes or electron donor-acceptor complexes. A general theory for charge-transfer complexes was formulated in 1952 by Mulliken.[1] According to this theory, the ground state wave function has the form

$$\psi_N = a\psi_0(D,A) + b\psi_1(D^+-A^-)$$

where $a \gg b$, $\psi(D,A)$ is the properly antisymmetrized no-bond wave function, and $\psi(D^+-A^-)$ represents transfer of an electron from the donor, D, to the acceptor, A. There is also an excited state

$$\psi_E = a^*\psi_1(D^+-A^-) - b^*\psi_0(D,A)$$

where $a^* \approx a$ and $b^* \approx b$.

This theory successfully explained many spectroscopic results. Mulliken also used the theory to predict the geometry of several types of charge-transfer complexes, among them the amine-halogen complexes.[2,3] Crystal structures determined by Hassel and co-workers and by other groups[4,5] were, however, not in agreement with these predictions. For complexes between lone-pair electron donors and halogens or other halogen-containing acceptors, the crystal structures showed that the geometry obeys quite simple rules and that the relative orientation of the partner molecules is very similar to that observed for hydrogen bonds.

The discrepancies between Mulliken's predictions and the crystal structures were among the reasons why it was argued and later generally accepted that it is not sufficient to consider only the charge-transfer interaction when describing the properties of the complexes and that in many complexes this interaction is not the dominant contribution to the ground-state stabilization.[6] The relative importance of the various contributions to this stabilization has been the subject of some dispute.[7]

A number of quantum mechanical works on charge-transfer complexes have been made in order to describe the nature of the intermolecular interactions. Morokuma and Kitaura[8] tried to separate the contributions from electrostatic, polarization, exchange, dispersion, and charge-transfer interactions. The sum of these contributions was, however, different from the calculated total energy, and an additional "mixing" term had to be added to account for this difference. In several works, attempts have been made to elucidate the similarity between charge-transfer and hydrogen bonds.[8-10] The results seem to disagree somewhat. Recently, a method of natural bond orbital analysis (NBO)[11-17] has been proposed for the study of intermolecular interactions. Compared with the Morokuma-Kitaura analysis, the NBO method leads to an alternative definition of the charge-transfer energy based on a different treatment of intermolecular overlap between filled and unfilled orbitals. The Morokuma-Kitaura approach and NBO analysis yield very different results for the charge-transfer energy, thereby illustrating some of the difficulties related to the charge-transfer concept.

The minimum energy N---halogen charge-transfer bond distances obtained by the quantum mechanical calculations are in general much longer than those found in the X-ray crystal structures.[8,10,16,18,19] It has been suggested that these differences are due to effects of the crystal forces in the X-ray structures.[10] Only two gas-phase structures of complexes between these kinds of molecules have been published. In the electron diffraction structure of the trimethylamine-bromine complex,[20] and extremely short N---Br bond and an unexpected orientation of the bromine molecule were observed. These results indicate that this complex is of a completely different type than ordinary charge-transfer complexes. In the microwave structure of the trimethylamine-trifluoroiodomethane complex,[21] the geometry of the charge-transfer bond is very close to that observed for similar complexes in the crystalline state. There are therefore no strong arguments for expecting a considerably longer charge-transfer bond distance in the gas phase than in the crystalline state.

The purpose of this work is 3-fold: (1) to demonstrate that accurate quantum chemical calculations on the complexes $H_3N{\cdot}F_2$, $H_3N{\cdot}Cl_2$, and $H_3N{\cdot}ClF$ yield nitrogen---halogen bond distances which are considerably shorter than the equilibrium distances obtained in previous calculations; (2) to analyze the differences

(1) Mulliken, S. R. *J. Am. Chem. Soc.* **1952**, *74*, 811.
(2) Mulliken, S. R. *J. Am. Chem. Soc.* **1950**, *72*, 600.
(3) Reid, C.; Mulliken, R. S. *J. Am. Chem. Soc.* **1954**, *76*, 3869.
(4) Hassel, O.; Rømming, C. *Q. Rev.* **1962**, *16*, 1.
(5) Prout, C. K.; Kamenar, B. In *Molecular Complexes*; Foster, R., Ed.; Elek: London, 1973; Vol. 1, Chapter 3.
(6) Hanna, M. W.; Lippert, J. L. In *Molecular Complexes*; Foster, R., Ed.; Elek: London, 1973; Vol. 1, Chapter 1.
(7) Mulliken, R. S.; Person, W. B. *J. Am. Chem. Soc.* **1969**, *91*, 3409.
(8) Morokuma, K.; Kitaura, K. In *Molecular Interactions*; Ratajczak, H., Orville-Thomas, W. J., Eds.; Wiley, New York, 1980; Vol. 1, Chapter 2.
(9) Kollman, P.; Allen, L. C. *Chem. Rev.* **1972**, *72*, 283.
(10) Kollman, P.; Dearing, A.; Kochanski, E. *J. Phys. Chem.* **1982**, *86*, 1607.
(11) Foster, J. P.; Weinhold, F. *J. Am. Chem. Soc.* **1980**, *102*, 7211.
(12) Weinstock, R. B. Ph.D. Thesis, University of Wisconsin—Madison. Weinstock, R. B.; Weinhold, F. University of Wisconsin Theoretical Chemistry Institute Report WIS-TCI-661, 1981.
(13) Reed, A. E.; Weinhold, F. *J. Chem. Phys.* **1983**, *78*, 4066.
(14) Reed, A. E.; Weinstock, R. B.; Weinhold, F. *J. Chem. Phys.* **1985**, *83*, 735.
(15) Curtiss, L. A.; Pochatko, D. J.; Reed, A. E.; Weinhold, F. *J. Chem. Phys.* **1985**, *82*, 2679.
(16) Reed, A. E.; Weinhold, F.; Curtiss, L. A.; Pochatko, D. J. *J. Chem. Phys.* **1986**, *84*, 5687.
(17) Reed, A. E.; Curtiss, L. A.; Weinhold, F. *Chem. Rev.* **1988**, *88*, 899.
(18) Lucchese, R. R.; Schaefer, H. F. *J. Am. Chem. Soc.* **1975**, *97*, 7205.
(19) Umeyama, H.; Morokuma, K.; Yamabe, S. *J. Am. Chem. Soc.* **1977**, *99*, 330.
(20) Shibata, S.; Iwata, J. J. *J. Chem. Soc., Perkin Trans. 2* **1985**, 9.
(21) Legon, A. C.; Millen, D. J.; Rogers, S. C. *Chem. Commun.* **1975**, 580.

0002-7863/92/1514-511$03.00/0

and the similarities of the bonding in these complexes; (3) on the basis of this analysis to suggest the characteristic features of electron donor–acceptor complexes.

The theoretical framework for our analysis is the extended geminal models developed by Røeggen.[22-28] These models are size-extensive, they can be applied for any intersystem distances, and they have a conceptual structure which facilitates interpretation. In particular, the energy decomposition scheme formulated within this framework shall be used to study the origin and the character of the interaction between the subsystems of the complexes in question.

The structure of the paper is as follows: In section II we give a brief description of the theoretical framework. Section III is devoted to computational details. In section IV we present the results and our analysis.

II. Theoretical Framework

In the works by Røeggen and co-workers[23,24,28] there is a detailed description of the theoretical approach adopted in this work. In this section we therefore give only the key ideas and the formulas required for the presentation of the results in section IV.

If the general extended geminal model[22] is truncated at the double-pair correction level, we have the following ansatz for the electronic wave function of a closed-shell $2N$-electron system:

$$\Phi^{\mathrm{EXG}} = \Phi^{\mathrm{APSG}} + \sum_{K=1}^{N} \Psi_K + \sum_{K<L}^{N} \Psi_{KL} \tag{1}$$

In eq 1 Φ^{APSG} denotes the APSG function, i.e., the antisymmetric product of strongly orthogonal geminals, Ψ_K represents a single-pair correction term, and Ψ_{KL} represents a double-pair correction term.

The energy can formally be evaluated within the framework of the method of moments:

$$\begin{aligned} E^{\mathrm{EXG}} &= \langle \Phi^{\mathrm{APSG}} | H \Phi^{\mathrm{EXG}} \rangle \\ &= E^{\mathrm{APSG}} + \sum_{K=1}^{N} \epsilon_K + \sum_{K<L}^{N} \epsilon_{KL} \end{aligned} \tag{2}$$

The difficult computational problem is the calculation of the double-pair correction terms $\{\epsilon_{KL}\}$. The numerical approximations involved are discussed in the recent works of Røeggen.[27,28]

The adopted approach yields geminals with charge densities localized in different parts of the physical space. To characterize the localization of the geminals, we introduce two concepts: the charge centroid and the charge ellipsoid of a geminal. The charge centroids are a set of vectors which are defined on the basis of the expression for the electronic part of the electric dipole moment. A straightforward derivation leads to the following well-known relation

$$\begin{aligned} \langle \Phi^{\mathrm{APSG}} | -\sum_{i=1}^{2N} r_i | \Phi^{\mathrm{APSG}} \rangle &= -\sum_{K=1}^{N} \int P_1^K(\mathbf{r})\, \mathbf{r}\, d\upsilon \\ &= -\sum_{K=1}^{N} 2 \int \tfrac{1}{2} P_1^K(\mathbf{r})\, \mathbf{r}\, d\upsilon = -\sum_{K=1}^{N} 2\mathbf{r}^K \end{aligned} \tag{3}$$

where $\mathbf{r}^K$ is the average position, or charge centroid, of the two electrons associated with the geminal Λ_K.

Following Robb et al.[29] and Csizmadia,[30] we define a measure of the extension of the geminal one-electron density by means of the second-order moments of the position operator, using the charge centroid as a local origin. The second-order moments (or variance matrix) are defined by the relations

$$M_{rs} = \tfrac{1}{2} \int [(x_r - x_r^K)(x_s - x_s^K)] P_1^K(\mathbf{r}')\, d\upsilon' \quad r, s \in \{1, 2, 3\} \tag{4}$$

wher x_r^K is the rth component of the charge centroid $\mathbf{r}^K$ defined in eq 3 and P_1^K is the one-electron density associated with the geminal Λ_K. If we diagonalize this symmetric variance matrix, we obtain what we may denote as a charge ellipsoid. The eigenvalues $\{a_1, a_2, a_3\}$ of the matrix (M_{rs}) correspond to the squares of the half-axes of the ellipsoid. The standard deviations in three orthogonal directions are therefore given by

$$\Delta l_i = \sqrt{a_i} \qquad i \in \{1, 2, 3\} \tag{5}$$

The quantities $\{\Delta l_i\}$ can then be used as a measure of the extension of the geminal one-electron density. Furthermore, we may also use the volume of the ellipsoid as a single number for the extension of the geminal one-electron density:

$$V = \frac{4\pi}{3} \Delta l_1 \Delta l_2 \Delta l_3 \tag{6}$$

By using the localization measures introduced in the previous paragraph, a molecular system can be partitioned into fragments or subsystems. Electron pairs and nuclei belonging to a given subsystem are localized in the same part of the physical space. In some recent works, Røeggen[23] and later Røeggen and Wisløff-Nilssen[24] have shown that the total electronic energy, i.e., the total energy in the absence of nuclear motion, can, within the framework of extended geminal models, be written as a sum of intra- and intersystem energies

$$\begin{aligned} E^{\mathrm{EXG}}_{\mathrm{supersystem}} &\equiv E^{\mathrm{EXG}} + E_{\mathrm{nuc}} \\ &= \sum_{\gamma} E^{\gamma} + \sum_{\gamma<\delta} E^{\gamma,\delta} \end{aligned} \tag{7}$$

where E^{EXG} is given by eq 2, E_{nuc} denotes the nuclear electrostatic energy, and E^{γ} and $E^{(\gamma,\delta)}$ are the intra- and intersystem energies, respectively. The intrasystem energy can be partitioned into kinetic, Coulombic, exchange, and correlation contributions:

$$E^{\gamma} = E^{\gamma}_{\mathrm{kin}} + E^{\gamma}_{\mathrm{coul}} + E^{\gamma}_{\mathrm{exch}} + E^{\gamma}_{\mathrm{corr}} \tag{8}$$

The intersystem energy between subsystems γ and δ is given by

$$E^{\gamma,\delta} = E^{\gamma,\delta}_{\mathrm{coul}} + E^{\gamma,\delta}_{\mathrm{exch}} + E^{\gamma,\delta}_{\mathrm{corr}} \tag{9}$$

As for the intermolecular potential U, we obtain a conceptually and physically very simple decomposition:

$$\begin{aligned} U &= E^{\mathrm{EXG}}_{\mathrm{supersystem}} - \sum_{\gamma} E^{\gamma}_{\mathrm{isolated}} \\ &= \sum_{\gamma} \{E^{\gamma}_{\mathrm{supersystem}} - E^{\gamma}_{\mathrm{isolated}}\} + \sum_{\gamma<\delta} E^{\gamma,\delta} \\ &= \Delta_{\mathrm{dist}} + \Delta_{\mathrm{int}} \\ &= \sum_{\gamma} \Delta^{\gamma}_{\mathrm{dist}} + \sum_{\gamma<\delta} \{\Delta^{\gamma,\delta}_{\mathrm{coul}} + \Delta^{\gamma,\delta}_{\mathrm{exch}} + \Delta^{\gamma,\delta}_{\mathrm{corr}}\} \end{aligned} \tag{10}$$

In the last equation, $\Delta^{\gamma}_{\mathrm{dist}}$ is the distortion energy of the subsystem γ due to the presence of the other subsystems. The interaction energy Δ_{int} is simply the sum of the Coulombic, exchange, and correlation parts in eq 10. It should be noted that the distortion energy Δ_{dist} is a repulsive term while the interaction terms are attractive. We shall denote the partitioning scheme expressed by eq 10 as the primary partitioning scheme within this framework.

A slightly modified version of the primary partition scheme might give further insight. It is based on two additional suppositions: First, the Coulombic energy is written as a sum of an electrostatic term and an induction term. Second, the exchange term $\Delta^{\gamma,\delta}_{\mathrm{exch}}$ is included in the distortion terms for the subsystems γ and δ.

The electrostatic subsystems $\Delta^{\gamma,\delta}_{\mathrm{elstat}}$ is simply defined as the Coulombic interaction between the undistorted subsystems for the given supersystem geometry. The induction energy is then defined as the difference between the Coulombic energy $\Delta^{\gamma,\delta}_{\mathrm{coul}}$ and $\Delta^{\gamma,\delta}_{\mathrm{elstat}}$; i.e.

(22) Røeggen, I. *J. Chem. Phys.* **1983**, *79*, 5520.
(23) Røeggen, I. *J. Chem. Phys.* **1986**, *85*, 262.
(24) Røeggen, I.; Wisløff-Nilssen, E. *J. Chem. Phys.* **1987**, *86*, 2869.
(25) Røeggen, I. *Int. J. Quantum Chem.* **1987**, *31*, 951.
(26) Røeggen, I. *J. Chem. Phys.* **1988**, *89*, 441.
(27) Røeggen, I. *Int. J. Quantum Chem.* **1990**, *37*, 585.
(28) Røeggen, I. *Mol. Phys.* **1990**, *70*, 353.
(29) Robb, M. A.; Haines, W. J.; Csizmadia, I. G. *J. Am. Chem. Soc.* **1973**, *95*, 42.
(30) Csizmadia, I. G. In *Localization and Delocalization in Quantum Chemistry*; Chalvet, O., Daudel, R., Diner, S., Malbrieu, J. P., Eds.; D. Reidel: Dordrecht, Holland, 1975.

$$\Delta^{\gamma,\delta}{}_{\text{ind}} = \Delta^{\gamma,\delta}{}_{\text{coul}} - \Delta^{\gamma,\delta}{}_{\text{elstat}} \tag{11}$$

Hence, the induction energy describes the changes in the Coulombic energy due to the rearrangement or distortion of the subsystems.

The second modification is related to the Pauli exclusion principle. Physically, we may interprete this principle as a prohibition for more than two electrons to occupy the same part of the physical space. Accordingly, when the subsystems are approaching each other, the electron pairs of each subsystem will be restricted in its movements since certain parts of the physical space are occupied by the electrons belonging to the other subsystems. The reduction in the effective physical space available for each electron pair leads to an increased kinetic energy, and therefore a positive distortion energy. The Pauli principle might therefore be considered as expressing a repulsive interaction between singlet coupled electron pairs. However, in our theoretical framework the effect of the Pauli principle is expressed in both the distortion energies and the terms which are explicitly denoted exchange terms. This decomposition of the effect of the Pauli principle is somewhat artificial and can be traced back to the strong orthogonality condition. The strong orthogonality condition implies that orbitals belonging to different geminals are orthogonal. This particular condition is imposed on the wave function in order to have tractable formulas. A simple product function of the type

$$\bar{\Phi} = \prod_{K=1}^{N} \Lambda_K \tag{12}$$

and with the strong orthogonality condition imposed does not satisfy the mathematical formulation of the Pauli principle. However, a determination of $\{\Lambda_K\}$ by minimizing the expectation value $\langle \bar{\Phi}|H\bar{\Phi}\rangle$ usually yields geminals that are essentially localized in separate parts of the physical space. The strong orthogonality condition has therefore a physical effect which is similar to the effect of the Pauli principle. However, the simple product function and the strong orthogonality conditions somewhat overestimate the physical separability of the electron pairs. When we introduce the Pauli principle in the proper way be means of the antisymmetrizer: i.e.

$$\Phi = M^{[N]}\mathcal{A}^{[2N]}\{\prod_{K=1}^{N} \Lambda_K\} \tag{13}$$

but still with the strong orthogonality condition imposed, we obtain a set of additional energy terms compared with the expectation value defined by the product function $\bar{\Phi}$.[22] These terms are denoted the exchange terms since they have their origin in the Pauli principle. The exchange terms are negative, showing that a simple product function with the strong orthogonality condition imposed is a somewhat too strong "physical" implementation of the Pauli principle. In our modified partitioning we shall include the complete effect of the Pauli principle in the distortion energies. We therefore define a set of modified distortion energies:

$$\tilde{\Delta}^{\gamma}{}_{\text{dist}} = \Delta^{\gamma}{}_{\text{dist}} + \tfrac{1}{2}\sum_{\delta \neq j} \Delta^{\gamma,\delta}{}_{\text{exch}} \tag{14}$$

As a result, we have the following modified decomposition scheme:

$$U = \sum_{\gamma} \tilde{\Delta}^{\gamma}{}_{\text{dist}} + \sum_{\gamma<\delta} (\Delta^{\gamma,\delta}{}_{\text{elstat}} + \Delta^{\gamma,\delta}{}_{\text{ind}} + \Delta^{\gamma,\delta}{}_{\text{corr}}) \tag{15}$$

In the terminology we are using in this work, there is a clear distinction between the intermolecular potential and the interaction energy between the subsystems. The intermolecular potential U is defined by the Born–Oppenheimer approximation. It is the effective potential that governs the motion of the *nuclei*. The interaction energy between the subsystems is the interaction energy between the subsystems including both *nuclei* and *electrons*. As expressed by eqs 10 and 15, the intermolecular potential can be expressed in terms of the distortion energies and the interaction energies between the subsystems.

III. Computational Details

The basis sets used in this study are constructed in the following way. For the chlorine atoms we start with Huzinaga's (12s, 9p) uncontracted

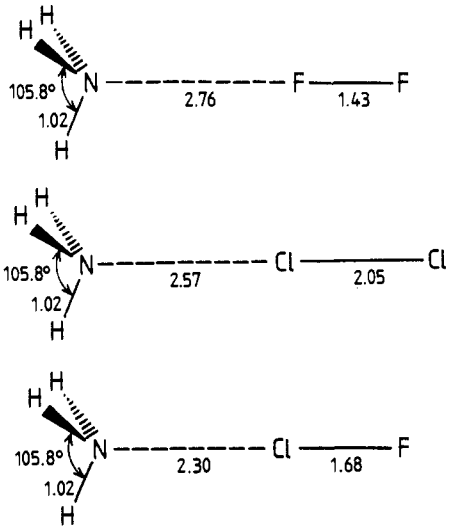

Figure 1. Equilibrium structures of the EDA complexes studied in this work (distances in angstroms).

Gaussian-type functions[31] contracted to [7s, 5p] as displayed in Table 17.12 in the compendium of Poirier et al.[32] The contracted set is augmented by two diffuse s-type functions and one set of diffuse p-type functions. The exponents of the diffuse functions are determined as an even-tempered extension of the original set. We add two sets of polarization functions. The first is appropriate for describing intraatomic correlation (exponents 0.68),[33] and the second is suitable for describing dispersion-type interactions (exponents 0.15).[34] The final basis set for the chlorine atoms is then [9s, 6p, 2d]. The basis set used for fluorine is a set of [7s, 4p, 2d] contracted Gaussian-type functions[28] and for hydrogen a [4s, 2p] set.[28] The basis for nitrogen, a [7s, 4p, 2d] contracted set, is constructed by exactly the same procedure as described by Røeggen.[28] The same set of polarization functions is adopted for fluorine and nitrogen.

In all calculations we are using the Beebe–Linderberg two-electron integral approximation.[35,36] We select an integral threshold of $\delta = 10^{-7}$ au. Test calculations on the HF molecule demonstrate that by using this integral threshold, the errors in the calculated energy should be less than 10^{-6} au.[36]

The bond pair geminals in F_2, ClF, and Cl_2 are described by two natural orbitals, while NH_3 is described by only RHF geminals in the root function.

In order to reduce the basis set superposition error (BSSE), we use the same procedure as advocated by Røeggen.[28] By following the recommendation by Schwenke and Truhlar,[37] we use as large a basis as we can afford and make no corrections at the RHF level. For the correlation terms the correction scheme is based on two assumptions: First, we neglect the intrasystem double-pair correction terms $\{\epsilon_{KL}\}$. Second, in calculating the single-pair correction terms $\{\epsilon_K\}$, we use exactly the same number of natural orbitals for the geminal of the isolated subsystem as for the corresponding geminal of the supersystem. Since the geminal one-electron density P_1^K (defined by a geminal Λ_K) is localized in a restricted part of the physical space and is only slightly distorted during formation of the dimer, the correlating orbitals will be more or less the same for the two cases considered. Hence, we can expect a small BSSE compared with a calculation of ϵ_K using the whole virtual orbital space for the supersystem. Adoption of this particular procedure for reducing the BSSE implies that the reported total energies, i.e., Table I, are somewhat artificially high since we have neglected the intrasystem double-pair correction terms.

The calculations are performed by using a numerical model denoted the EXGEM7 model. All intersystem double-pair correction terms $\{\epsilon_{KL}^{(2)}\}$ are defined in terms of 52 dispersion type natural orbitals (NO's).[26,27] The full CI corrections $\{\epsilon_{KL}^{(3)}\}$ are calculated in an orbital subspace consisting of 26 NO's. The full CI correction corresponds to, respectively,

(31) Huzinaga, S.; Arnau, C. *J. Chem. Phys.* **1970**, *53*, 348.
(32) Poirier, R.; Kari, R.; Csizmadia, I. G. *Physical Sciences Data 24, Handbook of Gaussian Basis Sets*; Elsevier: Amsterdam, 1985.
(33) Roos, B.; Siegbahn, P. *Theor. Chim. Acta* **1970**, *17*, 199.
(34) Krohn-Batenburg, L. M. J.; van Duijneveldt, F. B. *J. Mol. Struct.* **1985**, *121*, 185.
(35) Beebe, N. H. F.; Linderberg, J. *Int. J. Quantum Chem.* **1977**, *12*, 683.
(36) Røeggen, I.; Wisløff-Nilssen, E. *Chem. Phys. Lett.* **1986**, *132*, 154.
(37) Schwenke, D. W.; Truhlar, D. G. *J. Chem. Phys.* **1986**, *82*, 2418.

Table I. Total Energies of the Complexes $H_3N{\cdot}F_2$, $H_3N{\cdot}Cl_2$, and $H_3N{\cdot}ClF$ as a Function of the Nitrogen–Halogen Distance

complex	R/au	E^{APSG}/au	E^{EXGEM7} [a]/au
$H_3N{\cdot}F_2$	4.70	−255.027 764	−255.292 554
	5.20	−255.029 967	−255.293 318
	5.25	−255.030 069	−255.293 318
	5.33	−255.030 203	−255.293 306
	5.70	−255.030 505	−255.293 069
	∞	−255.029 368	−255.290 710
$H_3N{\cdot}Cl_2$	4.75	−975.212 342	−975.510 398
	4.85	−975.213 418	−975.510 447
	4.95	−975.214 273	−975.510 403
	∞	−975.212 612	−975.501 091
$H_3N{\cdot}ClF$	4.20	−615.132 534	−615.427 704
	4.30	−615.134 584	−615.427 822
	4.40	−615.136 220	−615.427 806
	4.50	−615.137 505	−615.427 564
	4.60	−615.138 494	−615.427 269
	∞	−615.133 360	−615.410 665

[a] Intrasystem double-pair correction terms $\{\epsilon_{KL}\}$ are neglected.

Table II. Equilibrium Distances and Binding Energies for the Complexes $H_3N{\cdot}F_2$, $H_3N{\cdot}Cl_2$, and $H_3N{\cdot}Cl_F$

	$H_3N{\cdot}F_2$		$H_3N{\cdot}Cl_2$		$H_3N{\cdot}ClF$	
model	R_e/Å	D_e/kJ mol^{-1}	R_e/Å	D_e/kJ mol^{-1}	R_e/Å	D_e/kJ mol^{-1}
SCF [DZ][a]	3.08	2.5	2.93	10.0	2.65	32.0
SCF [DZ + 1d][a]	3.04	3.3			2.62	31.0
SCF [4-31G][b]	3.00	4.4	2.93	12.1	2.72	34.4
MP2/6-31G*[c]	2.60	10.53				
present work EXGEM7[9s,6p,2d/7s,4p,2d/4s,2p]	2.76	6.8	2.57	24.6	2.30	45.1

[a] Lucchese, R. R.; Schaefer, H. F. III *J. Am. Chem. Soc.* **1975**, *97*, 7205. [b] Umeyama, H.; Morokuma, K.; Yamabe, S. *J. Am. Chem. Soc.* **1977**, *99*, 330. [c] Reed, A. E.; Weinhold, F.; Curtiss, L. A.; Pochatko, D. J. *J. Chem. Phys.* **1986**, *84*, 5687.

29.7%, 27.5%, and 24.6% of the total intersystem correlation energy for $H_3N{\cdot}F_2$, $H_3N{\cdot}Cl_2$, and $H_3N{\cdot}ClF$.

IV. Results

(A) Equilibrium Structures. The equilibrium geometries of the complexes are depicted in Figure 1. The geometries of the isolated monomers are optimized. The geometries of the complexes are obtained by a partial geometry optimization. For all complexes a C_{3v} symmetry is assumed. This is in accordance with the results of the calculations of Umeyama et al.[19] and with all crystal structures of amine–halogen complexes investigated so far.[5,38] The geometries of the monomers are assumed to be unchanged upon complex formation. Accordingly, for the complexes we minimize the energy with respect to one geometrical parameter, the nitrogen–halogen distance, i.e., the distance between the nitrogen nucleus and the halogen nucleus which is closest to the nitrogen nucleus. In Table I we present total electronic energies, i.e., the total energies in the absence of nuclear motion, as a function of this distance. The equilibrium distance and binding energy for each complex are obtained by a parabolic fit, and the results are displayed in Table II.

For the complex $H_3N{\cdot}ClF$ the difference between the equilibrium nitrogen–chlorine distance and the distance R = 4.30 au is only 0.04 au. The energy difference between these two points on the potential surface is less than 0.000 01 au. We have therefore not considered it necessary to perform a new calculation corresponding to the equilibrium distance. Accordingly, all detailed numerical results pertaining to this complex refer to a nitrogen–chlorine distance of 4.30 au.

The only previously published ab initio calculations on these three complexes are the works of Lucchese et al.[18] and Umeyama et al.[19] at the SCF level. In addition, there exists a MP2 calculation of Reed et al.[16] on $H_3N{\cdot}F_2$. For comparison, the results

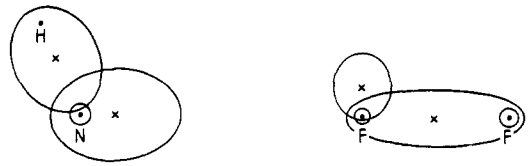

Figure 2. Intersection between the xy plane and selected charge ellipsoids of $H_3N{\cdot}F_2$. The hydrogen nuclei of NH_3 are rotated to eclipsed configuration with respect to the lone pair ellipsoids of the electron pair accepting fluorine nucleus; otherwise, the geometry is equal to the equilibrium geometry as determined in this work. Charge centroids are marked with a cross (×) and nuclear positions with a dot (●). (The xy plane is defined by the nitrogen nucleus, a halogen, and a hydrogen nucleus.)

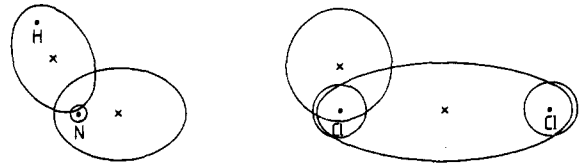

Figure 3. Intersection between the xy plane and selected charge ellipsoids of $H_3N{\cdot}Cl_2$. The core electron pairs of the chlorine atoms are represented by the smallest spherical surface enclosing the core electron pair ellipsoids. The hydrogen nuclei of NH_3 are rotated to eclipsed configuration with respect to the lone pair ellipsoids of the electron pair accepting chlorine nucleus; otherwise, the geometry is equal to the equilibrium geometry as determined in this work. Charge centroids are marked with a cross (×) and nuclear positions with a dot (●). (The xy plane is defined by the nitrogen nucleus, a halogen, and a hydrogen nucleus.)

of their calculations are also included in Table II.

There are some striking differences between the SCF calculations and the present study. We obtain both shorter equilibrium distances and larger binding energies. This is expected since the intersystem correlation term has an attractive character. This effect is also clearly demonstrated in the MP2 calculation of Reed et al. on $H_3N{\cdot}F_2$. A second reason for the difference in question is the far more flexible basis sets which are used in the present work. The discrepancy between the quoted MP2 calculation and our calculation on $H_3N{\cdot}F_2$ is most likely due to a considerably larger BSSE in the work by Reed et al. In a series of calculations on the water dimer using a variety of basis sets, Reed et al.[16] showed that a 6-31G* basis set might yield a BSSE at the RHF level of the order of 4–6 kJ mol^{-1}. In addition, the uncorrected MP2 correlation energy in their work will also yield a substantial contribution to the BSSE.

There are no experimental results for equilibrium distances or binding energies for the complexes studied in this work. However, an N···Br distance of 2.16 Å has been observed in the crystal structure of an amine–Br_2 complex.[38] In the dioxane complexes of Br_2[39] and Cl_2,[40] the oxygen–halogen distances are approximately equal. It is therefore unreasonable to expect N···Cl much longer than 2.2 Å in the $H_3N{\cdot}Cl_2$ complex. According to this reasoning, our calculated intersystem distances are still somewhat too large. This should also be the case since our basis set is far from complete. A further extension of the basis set will increase the magnitude of the intersystem correlation energy and reduce the nitrogen–halogen distances.

The equilibrium distance and the binding energy, respectively, decrease and increase when we follow the sequence $H_3N{\cdot}F_2$, $H_3N{\cdot}Cl_2$, and $H_3N{\cdot}ClF$. This agrees well with results obtained spectrophotometrically for complexes of Br_2, I_2, ICl, and IBr in solution: The stability of the complexes increases with increasing atomic number of the halogens, and the heteronuclear molecules form more stable complexes than homonuclear molecules.[41] This qualitative trend can be easily understood when we look at the properties of the subsystems. We may take as a basic supposition

(38) Eia, G.; Hassel, O. *Acta Chem. Scand.* **1956**, *10*, 139.

(39) Hassel, O.; Hvoslef, J. *Acta Chem. Scand.* **1954**, *8*, 873.
(40) Hassel, O.; Hvoslef, J. *Acta Chem. Scand.* **1956**, *10*, 138.
(41) Foster, R. *Organic Charge-transfer Complexes*; Academic Press: London, New York, 1969; p 201.

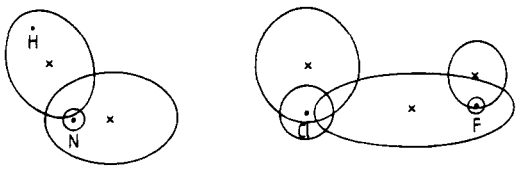

Figure 4. Intersection between the *xy* plane and selected charge ellipsoids of $H_3N{\cdot}ClF$. The core electron pairs of the chlorine atoms are represented by the smallest spherical surface enclosing the core electron pair ellipsoids. The hydrogen nuclei of NH_3 are rotated to eclipsed configuration with respect to the lone pair ellipsoids of the chlorine nucleus; otherwise, the geometry is equal to the equilibrium geometry as determined in this work. Charge centroids are marked with a cross (×) and nuclear positions with a dot (●). (The *xy* plane is defined by the nitrogen nucleus, a halogen, and a hydrogen nucleus.)

Table III. Electric Dipole Moments of the Isolated Monomers and the Differences between the Corresponding Quantities in the Complex and the Isolated Monomer[a]

complex	monomer	d^{mon}	$d^{comp} - d^{mon}$
$H_3N{\cdot}F_2$	NH_3	0.6563	0.0240
	F_2	0.0	0.0807
$H_3N{\cdot}Cl_2$	NH_3	0.6563	0.2545
	Cl_2	0.0	0.4110
$H_3N{\cdot}ClF$	NH_3	0.6563	0.5149
	ClF	0.3409	0.3987

[a] Dipole moments in au.

that the binding of a complex is essentially due to electrons of one subsystem approaching the nuclei of another subsystem. This conjecture is supported by the energy decomposition analysis to be presented in subsection C. By choosing this particular premise, we infer that the binding energy depends both on how well a nucleus of the acceptor subsystem is screened by the electrons attached to it and the character of the donated electron pair. Since we for the complexes in question have the same donor, the differences in equilibrium structures must be attributed to the acceptor subsystems. In Figures 2–4 we display the intersection between selected charge ellipsoids of the three complexes and a symmetry plane passing through the nitrogen–halogen axis. From these figures we can discern that the fluorine nucleus is more effectively screened by the lone pairs attached to it than what is the case for the more bulky chlorine atom. Accordingly, we should expect that the lone pair of ammonia is experiencing a larger force from the screened chlorine nucleus than from the screened fluorine nucleus. Furthermore, the bond pair of ClF is screening the chlorine nucleus in a less effective way compared with the screening by the bond pair of a chlorine nucleus of Cl_2. This feature explains qualitatively why the distance is shorter and the binding energy is larger in $H_3N{\cdot}ClF$ than in $H_3N{\cdot}Cl_2$. In this qualitative reasoning we have stressed what we consider to be the main effects. However, the Coulombic interactions of the Hamiltonian clearly emphasize that a quantitative explanation must take into account not only the main "actors" but all the entities of the subsystems. Nevertheless, we believe that a pictorial analysis of the type given might give valuable insight.

(B) Changes of the One-Electron Density. As an overall measure of the changes of the one-electron density during complex formation, we consider the changes of the electric dipole moments of the subsystems. The electric dipole moments are calculated at the APSG level and are presented in Table III.

For all complexes there is a shift of the electronic charge density along the complex axis in the direction from nitrogen to halogen. All subsystem shifts have the same sign. As for the donor subsystem, there is only a small change for the complex $H_3N{\cdot}F_2$ and approximately 10 and 20 times larger for $H_3N{\cdot}Cl_2$ and $H_3N{\cdot}ClF$, respectively. Concerning the acceptor subsystems, the change is smallest for F_2 and considerably larger for Cl_2 and ClF. A more detailed picture of changes of the density can be obtained if we look at the changes of the charge centroids of the geminals. The changes of the *x* components (bond axis) of some selected charge centroids are given in Table IV. As we could expect intuitively, the largest shift in the donor subsystem is found for the lone pair

Table IV. Changes of the *x* Components of the Charge Centroids of Selected Geminals of the Complexes $H_3N{\cdot}F_2$, $H_3N{\cdot}Cl_2$, and $H_3N{\cdot}ClF$ Compared with the Corresponding Quantities of the Isolated Monomers[a,b]

complex	geminal	x^K
$H_3N{\cdot}F_2$	bond pair of F_2	0.0058
	lone pair associated with F_α	0.0077
	lone pair associated with F_b	0.0037
	lone pair of N	0.0086
	bond pair of NH_3	0.0012
$H_3N{\cdot}Cl_2$	bond pair of Cl_2	0.0441
	lone pair associated with Cl_α	0.0359
	lone pair associated with Cl_b	0.0177
	lone pair of N	0.0956
	bond pair of NH_3	0.0105
$H_3N{\cdot}ClF$	bond pair of ClF	0.0385
	lone pair associated with Cl	0.0366
	lone pair associated with F	0.0173
	lone pair of N	0.1994
	bond pair of NH_3	0.0192

[a] *x* components in au. Direction of *x*-axis from nitrogen to halogen atom. [b] Subscript a is used on the nucleus of the halogen molecule, which is closest to the nitrogen nucleus.

Table V. Half-Axes and Volume of the Charge Ellipsoid of the Lone Pair Geminal of Isolated NH_3 and the Corresponding Lone Pair Geminal in the Complexes $H_3N{\cdot}F_2$, $H_3N{\cdot}Cl_2$, and $H_3N{\cdot}ClF$ (Differences in Quantities with Respect to the Values for the Isolated Subsystem in Parentheses)[a]

system	Δl_x	Δl_y	Δl_z	V
isolated NH_3	1.1073	0.8563	0.8563	3.4010
$H_3N{\cdot}F_2$	1.1088	0.8526	0.8526	3.3762
	(0.0015)	(−0.0037)	(−0.0037)	(−0.0248)
$H_3N{\cdot}Cl_2$	1.1975	0.8389	0.8389	3.5305
	(0.0902)	(−0.0174)	(−0.0174)	(0.1295)
$H_3N{\cdot}ClF$	1.2500	0.8218	0.8218	3.5360
	(0.1427)	(−0.0345)	(−0.0345)	(0.1350)

[a] Distances and volumes in atomic units.

Table VI. Half-Axes and Volume of the Charge Ellipsoid of the Bond Pair Geminal of the Acceptor Subsystem in the Complexes $H_3N{\cdot}F_2$, $H_3N{\cdot}Cl_2$, and $H_3N{\cdot}ClF$ (Differences of Quantities with Respect to the Values for the Isolated Subsystem in Parentheses)[a]

system	Δl_x	Δl_y	Δl_z	V
$H_3N{\cdot}F_2$	1.6266	0.5354	0.5354	1.9480
isolated	1.6392	0.5327	0.5327	1.9485
complex	(0.0166)	(−0.0027)	(−0.0027)	(0.0005)
$H_3N{\cdot}Cl_2$	2.3442	0.8505	0.8505	7.1034
isolated	2.4174	0.8464	0.8464	7.2533
complex	(0.0732)	(−0.0041)	(−0.0041)	(0.1499)
$H_3N{\cdot}ClF$	1.8167	0.6647	0.6647	3.3623
isolated	1.9418	0.6532	0.6532	3.4702
complex	(0.1251)	(−0.0115)	(−0.0115)	(0.1079)

[a] Distances and volumes in atomic units.

geminal. Similarly, the bond pair and the lone pairs of the halogen atom closest to the nitrogen nucleus are mostly affected in the acceptor subsystem. A still more detailed picture can be obtained by examining the charge ellipsoids. In Table V we give details for the donor lone pair ellipsoid. We notice that for all three complexes there is an expansion along the nitrogen–halogen bond axis and a contraction in the two orthogonal directions. This effect is consistent with the picture of the bonding given in the previous subsection; i.e., the bonding is due to the lone pair of nitrogen approaching a nucleus of the acceptor. In Table VI data are given for the charge ellipsoid of the bond pair of the acceptor subsystems. The pattern of change is the same as for the lone pair ellipsoid of the donor: expansion along the bond axis and contraction along the directions orthogonal to the bond axis.

(C) Energy Decomposition. In Table VII we present the results based on our primary decomposition scheme. There are some striking features in this table: First, the dominant terms for a complex are the Coulombic term, the distortion terms, and the exchange term. However, these terms partly cancel on summation.

Table VII. Partitioning of the Intermolecular Potential Using the Primary Partitioning Scheme (Numbers in Parentheses Based on the Sum of the Repulsive Terms as Energy Unit)[a]

	$H_3N{\cdot}F_2$	$H_3N{\cdot}Cl_2$	$H_3N{\cdot}ClF$
Δ^{a}_{dist}	0.014 075	0.107 272	0.226 300
	(55.2%)	(62.5%)	(57.2%)
Δ^{d}_{dist}	0.011 404	0.064 316	0.169 496
	(44.8%)	(37.5%)	(42.8%)
$\Delta^{a,d}_{coul}$	−0.020 037	−0.132 945	−0.314 220
	(−78.6%)	(−77.5%)	(−79.4%)
$\Delta^{a,d}_{exch}$	−0.005 880	−0.036 604	−0.078 593
	(−23.1%)	(−21.3%)	(−19.9%)
$\Delta^{a,d}_{corr}$	−0.002 170	−0.011 406	−0.020 139
	(−8.5%)	(−6.6%)	(−5.1%)
U	−0.002 608	−0.009 367	−0.017 156
	(−10.2%)	(−5.5%)	(−4.3%)

[a] Atomic units.

Table VIII. Partitioning of the Intermolecular Potential Using the Modified Partitioning Scheme (Numbers in Parentheses Based on the Sum of the Repulsive Terms as Energy Unit)[a]

	$H_3N{\cdot}F_2$	$H_3N{\cdot}Cl_2$	$H_3N{\cdot}ClF$
$\tilde{\Delta}^{a}_{dist}$	0.011 135	0.088 970	0.187 004
	(56.8%)	(65.9%)	(59.0%)
$\tilde{\Delta}^{d}_{dist}$	0.008 464	0.046 014	0.130 200
	(43.2%)	(34.1%)	(41.0%)
$\Delta^{a,d}_{elstat}$	−0.003 773	−0.024 441	−0.057 786
	(−19.3%)	(−18.1%)	(−18.2%)
$\Delta^{a,d}_{ind}$	−0.016 264	−0.108 504	−0.256 434
	(−83.0%)	(−80.4%)	(−80.8%)
$\Delta^{a,d}_{corr}$	−0.002 170	−0.011 406	−0.020 139
	(−11.1%)	(−8.5%)	(−6.3%)
U	−0.002 608	−0.009 367	−0.017 156
	(−13.3%)	(−6.9%)	(−5.4%)

[a] Atomic units.

Accordingly, the intersystem correlation term, which in magnitude is considerably smaller, is of paramount importance for the potential. Second, the Coulombic term has the far largest magnitude of the attractive terms. It is therefore appropriate to consider it as the main origin of the interaction. In Table VIII the Coulombic term is partitioned into electrostatic and induction components. We notice that for all three complexes the induction component is approximately 4 times larger than the electrostatic component.

For comparison we have applied the modified partitioning scheme to the hydrogen-bonded complexes $(HF)_2$, $(H_2O)_2$, and $H_2O{\cdot}HF$. The adopted basis sets and the computational model are as described in the work of Røeggen.[28] All calculations refer to the equilibrium geometry as determined in the quoted work. The results of the partitioning are displayed in Table IX. We notice in particular that even though the magnitude of the induction term is larger than the magnitude of the electrostatic term also for the hydrogen-bonded complexes, the ratio $\Delta_{ind}/\Delta_{elstat}$ is considerably smaller than for the studied EDA complexes. We shall therefore put forward a conjecture that the main difference between EDA complexes and hydrogen-bonded systems is related to the different relative importance of the electrostatic and the inductive components of the potential.

The energy partitioning supports our previously formulated conjecture concerning the binding of these complexes: To reduce the exclusion repulsion due to the Pauli principle and to have a favorable electrostatic interaction, the donor lone pair approaches the "vacant" space in the vicinity of a nucleus of the acceptor. During the process there is a shift of the charge densities in the direction from donor to acceptor in both the donor and the acceptor. This shift of charge densities is the origin of the large induction energy which is the main component of the interaction energy.

Table IX. Partitioning of the Intermolecular Potential for Hydrogen-Bonded Systems Using the Modified Partitioning Scheme (Numbers in Parentheses Based on the Sum of the Repulsive Terms as Energy Unit)[a,b]

	HF·HF	$H_2O{\cdot}H_2O$	$H_2O{\cdot}HF$
$\tilde{\Delta}^{a}_{dist}$	0.010 537	0.011 504	0.022 087
	(42.3%)	(43.3%)	(38.7%)
$\tilde{\Delta}^{d}_{dist}$	0.014 360	0.015 085	0.034 933
	(57.7%)	(56.7%)	(61.3%)
$\Delta^{a,d}_{elstat}$	−0.012 935	−0.013 479	−0.023 782
	(−52.0%)	(−50.7%)	(−41.7%)
$\Delta^{a,d}_{ind}$	−0.017 137	−0.018 091	−0.043 160
	(−68.8%)	(−68.0%)	(−75.7%)
$\Delta^{a,d}_{corr}$	−0.002 270	−0.003 246	−0.004 590
	(−9.1%)	(−12.2%)	(−8.0%)
U	−0.007 445	−0.008 227	−0.014 512
	(−29.9%)	(−30.9%)	(−25.5%)

[a] Atomic units. [b] Equilibrium geometry as determined by Røeggen.[28]

If we look at the rescaled energy decomposition by using for each complex the sum of the repulsive components as the energy unit, we discover a remarkable similarity. In our primary partitioning scheme (Table VII), the relative importance of the Coulombic and exchange terms is more or less the same for all three complexes. The modified partitioning scheme (Table VIII) discloses a similar pattern for the electrostatic and induction terms of these complexes. The rescaled distortion energies have a somewhat larger variation but are still quite similar.

V. Concluding Remarks

In this work we have clearly demonstrated that accurate quantum chemical calculations on the complexes $H_3N{\cdot}F_2$, $H_3N{\cdot}Cl_2$, and $H_3N{\cdot}ClF$ yield considerably shorter nitrogen-halogen equilibrium distances than what is previously reported (except for the quoted MP2 calculation on $H_3N{\cdot}F_2$ by Reed et al.[16]). The adopted energy decomposition scheme has displayed the similarity and differences between the three complexes. In particular, we emphasize the role of the Coulombic interaction as the main origin of the intermolecular interaction. The difference between this kind of EDA complex and hydrogen-bonded complexes seems to be related to the different relative importance of the electrostatic and inductive components of the potential.

In a forthcoming work we shall present similar calculations on the strongly bonded EDA complexes $H_3B{\cdot}CO$ and $H_3B{\cdot}NH_3$. As a result of some preliminary calculations we can report that the qualitative pattern of bonding in these two complexes, i.e., by using rescaled energy components, is very similar to the results reported for the more weakly bonded EDA complexes studied in this work.

Acknowledgment. We thank J. Almlöf for giving access to his integral program MOLECULE. All calculations reported in this work were performed on the Cray X-MP216 supercomputer at RUNIT, Trondheim, Norway. This work was supported by the Norwegian Research Council for Science and the Humanities.

Registry No. NH_3, 7664-41-7; F_2, 7782-41-4; Cl_2, 7782-50-5; ClF, 7790-89-8.